# Structural Evaluation of Concrete Pavements Based on Static and Dynamic Backanalysis

Kunihito Matsui[1], James W. Maina[2] and Tatsuo Nishizawa[3]

## Abstract

Statistical characteristics of falling weight deflectometer (FWD) deflections and the backcalculated moduli were investigated based on the data obtained from FWD tests conducted on the newly constructed concrete pavements. The precise statistical evaluation was performed for uniform section that was identified based on AASHTO method. Statistical parameters of FWD deflections and layer moduli for uniform sections of sound concrete pavement structures were obtained. It was found that stiffness of subbase and subgrade strongly affect uniformity of FWD deflection for a pavement section and that the frequency distributions of the deflection and backcalculated moduli can be approximated by normal probability functions.

## Introduction

In order to evaluate structural soundness of concrete pavements, statistical characteristics of FWD deflections and backcalculated moduli should be known. One type of concrete pavement is JPCP (Jointed Plain Concrete Pavement), which has many slabs connected with each other by doweled joints. There might be differences in structural conditions among the slabs and joints. These differences are caused very likely by variations in thickness of concrete and subbase and/or compaction of subbase and subgrade. It is important to know the initial condition of concrete pavement to follow up its integrity. In this study, FWD measurements were conducted on newly constructed concrete pavement sections. The sections are comprised of a jointed concrete pavement section (Section A). In these sections, numerous FWD tests were performed in order to collect as many deflection data as possible. Statistical parameters were estimated from these data and discussed in terms of the statistical characteristics of FWD deflections and backcalculated moduli.

## FWD Measurement

Sections on which FWD tests were performed are located on a national road. Details of the 700m long Section A with doweled joints are as shown in **Table 1**.

[1] Professor, Department of Civil Engineering, College of Science and Engineering, Tokyo Denki University, Hatoyama-cho, Hiki-gun, Saitama, 350-0394, Japan (matsui@g.dendai.ac.jp)
[2] Visiting Scholar, Department of Civil Engineering, College of Science and Engineering, Tokyo Denki University, Hatoyama-cho, Hiki-gun, Saitama, 350-0394, Japan (mainajw@g.dendai.ac.jp)
[3] Professor, Ishikawa National College of Technology, Tsubata, Ishikawa, 929-0392, Japan (nishi@ishikawa-nct.ac.jp)

**Table 1. Pavement Construction Details.**

| Layer | Jointed Concrete Pavement Section A |
|---|---|
| Concrete Slab | 30cm |
| Asphalt Interlayer | 4cm |
| Granular subbase | 15cm |
| CBR of Subgrade | 12% |
| Joint Spacing | 10m |

The time of the FWD test was from November 30, 2000 to December 1, 2000. The FWD loading plate diameter was 300 mm and the magnitude of the load was 98kN (10tf). Deflections were measured at 0, 20, 30, 45, 60, 90 and 120 cm from the center of the loading plate and referred to as D0, D20, D30, D45, D60, D90 and D120, respectively. Four load drops were applied at each measurement point. The first reading was omitted and the remaining three readings were averaged to obtain a representative deflection basin for the measurement point. To eliminate effects of small variations in the applied load, all averaged deflections were normalized to the ones of a standard load of 98 kN. The following measurement points were selected. In Section A, measuring points were the center of all 74 slabs and at all joint edges. In a joint edge measurement, the load plate was located at the joint edge and the deflection sensors except for D0 were located on the unloaded slab across the joint to estimate load transfer efficiency (LTE).

Along with the FWD tests, thermocouples were embedded in the concrete slab and concrete slab and air temperatures were measured. Joint opening at each joint was also recorded.

In order to compare results of static and dynamic backcalculation analyses, time series data were collected at a single measurement point.

## Temperature Condition

Variations of the temperatures in the concrete slab and the air temperature during the testing days are shown in **Figure 1**. On the first day, the weather was cloudy and the temperature in the concrete slab was relatively low. The measurements were completed by noon on the second day when the weather recovered but the temperature at the pavement surface was still only 15 $^{o}$C. **Figure 2** shows a variation of temperature gradient in the concrete slab that is defined as the temperature differential between the top and bottom of the slab divided by the slab thickness. The temperature gradient was less than 0.2 $^{o}$C/cm from the first day to 0.3 $^{o}$C/cm around 11:00 a.m. on the second day when most measurements were done. The effect of temperature gradient is supposed to be very little on FWD deflections of concrete pavement if it is less than 0.2 $^{o}$C/cm. Therefore, the effect of temperature gradient on FWD deflections was neglected in this study.

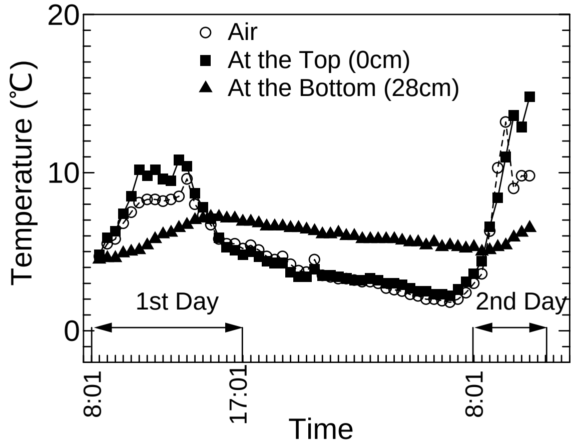


**Figure 1. Temperature Variations.**

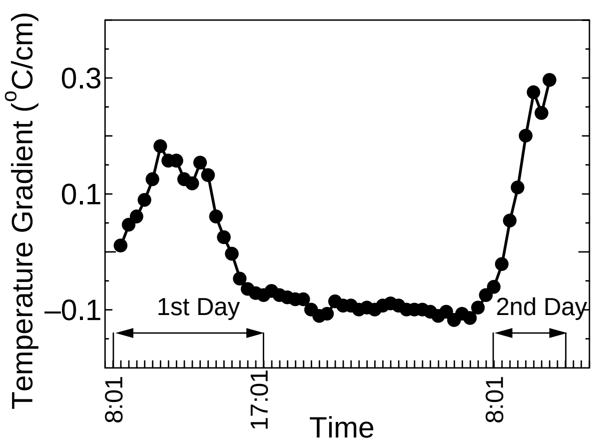


**Figure 2. Variation of Temperature Gradient.**

**FWD Measurement Results**

Variations of FWD deflections measured in Section A are shown in **Figure 3**. In this figure, D0, D30, D60, and D120 are plotted along the distance. It seems that the section can be divided into several uniform subsections. AASHTO guide proposes a method to divide a measured section into uniform subsections using accumulated deflection differential, *Zx* (AASHTO, 1986).

**Figure 4** shows *Zx* along the distance in Section A. A point at which gradient of Zx changes from negative to positive or from positive to negative is supposed to be a border of a uniform subsection. Based on this method, Section A was divided into 3 uniform subsections (A-1, A-2 and A-3) as shown in Figure 3. The A-3 section was excluded from the following discussion, because the number of points was too small.

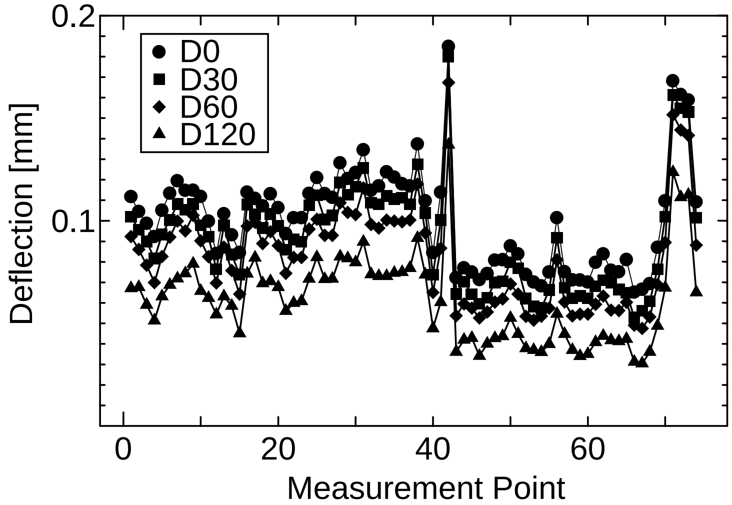


**Figure 3. Variations of FWD Deflections along Distance for Section A.**

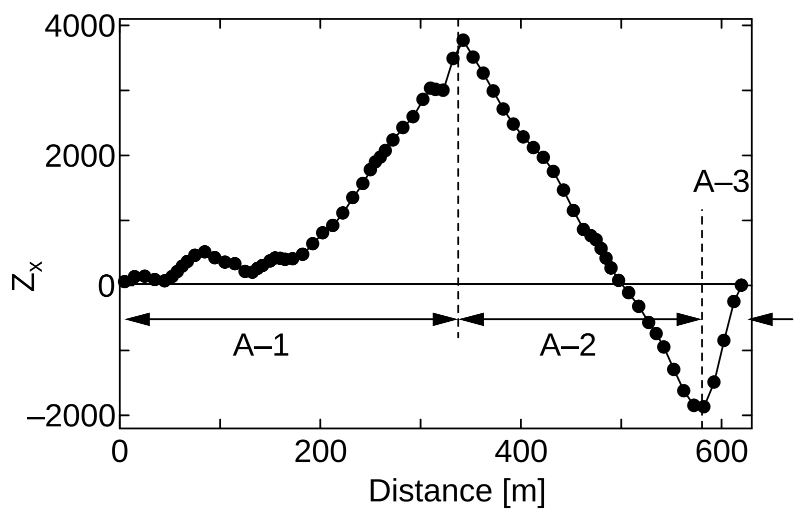


**Figure 4. Accumulated Deflection Differential Zx for Section A.**

**Table 2** summarizes statistical parameters in Section A for all deflections, and the deflections in the subsections, A-1 and A-2, respectively. For all deflections, the coefficient of variance (COV) ranged from 24% to 30 % for sensors near the loading plate and more than 30 % for sensors far from the loading plate. On the other hand, for subsections A-1 and A-2, COV decreased down to 10 % ~ 18% in all sensors. Therefore, it can be said that COV for sound jointed concrete pavement structures, like newly constructed ones, would range from 10 % up to 18 %. As far as D0 is concerned, its COV would be estimated roughly to about 10 %.

**Table 2. Statistical Parameters of FWD Deflections for Section A.**

| | Sensor | D0 | D20 | D30 | D45 | D60 | D90 | D120 |
|---|---|---|---|---|---|---|---|---|
| All | Average (mm) | 0.101 | 0.096 | 0.092 | 0.087 | 0.082 | 0.071 | 0.062 |
| | Standard Deviation (mm) | 0.025 | 0.026 | 0.026 | 0.026 | 0.025 | 0.024 | 0.022 |
| | COV | 0.249 | 0.270 | 0.284 | 0.292 | 0.305 | 0.341 | 0.354 |
| A-1 | Average (mm) | 0.110 | 0.105 | 0.101 | 0.096 | 0.091 | 0.079 | 0.069 |
| | Standard Deviation (mm) | 0.011 | 0.012 | 0.012 | 0.012 | 0.012 | 0.011 | 0.010 |
| | COV | 0.104 | 0.117 | 0.116 | 0.121 | 0.126 | 0.139 | 0.139 |
| A-2 | Average (mm) | 0.078 | 0.073 | 0.068 | 0.064 | 0.059 | 0.049 | 0.041 |
| | Standard Deviation (mm) | 0.010 | 0.011 | 0.010 | 0.010 | 0.009 | 0.009 | 0.008 |
| | COV | 0.128 | 0.146 | 0.154 | 0.152 | 0.153 | 0.178 | 0.185 |

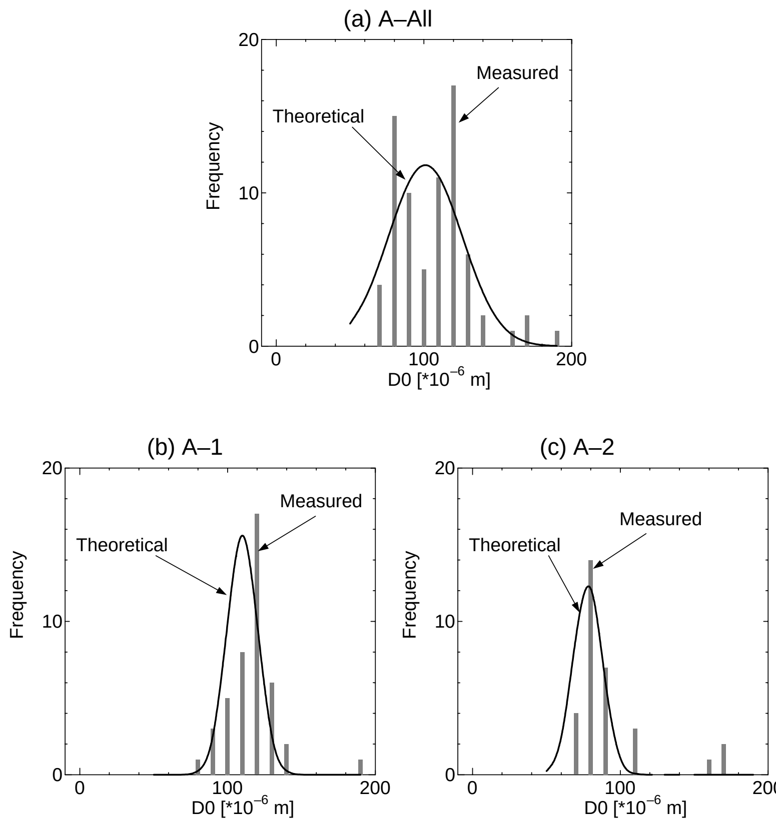


**Figure 5. Histograms for D0 for Section A.**

**Figures 5(a)** to **5(c)** show histograms for all deflections in Section A and the subsections A-1 and A-2, respectively. In **Figure 5(a)** two peaks in the frequency distribution can be seen, suggesting that Section A had at least two uniform subsections. If uniform subsections can be properly identified, the frequency distribution for each subsection can be approximated by a normal (Gaussian) probability distribution function as shown in **Figures 5(b**) and **5(c)**.

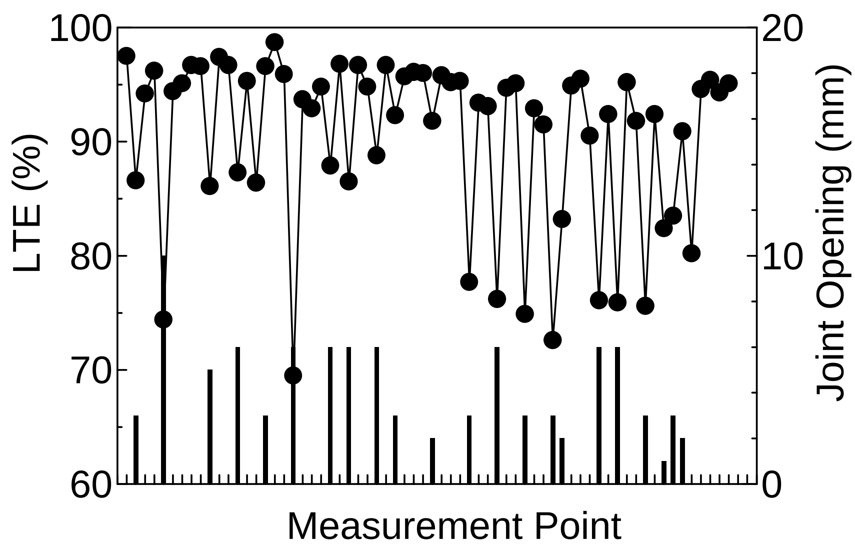


**Figure 6. Variations of LTE and Width of Joint Opening along Distance for Section A.**

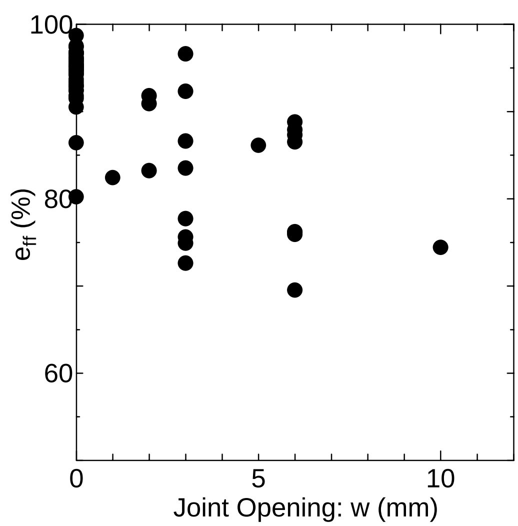


**Figure 7. Relationship between LTE and Width of Joint Opening.**

The load transfer efficiency (LTE) at doweled transverse joint was estimated as follows:

$$e_{ff} = \frac{D30}{(D0 + D30)/2} \times 100 \ (\%)$$

**Figure 6** summarizes LTE for Section A and joint opening along the distance. LTE showed large variation, because cracks did not occur at some of the transverse joints at the time of the test. It seems that low LTE appeared at the joints with wide crack openings. The average and COV of LTE in this section were 90.9% and 7.8 %, respectively. Relationship between LTE and the width of joint opening is shown in

**Figure 7**. Although LTE was less than 80 % when the width of joint opening was more than 3mm, there is no clear correlation between them. This means that the dowel bars at the joint worked very well for the load transfer.

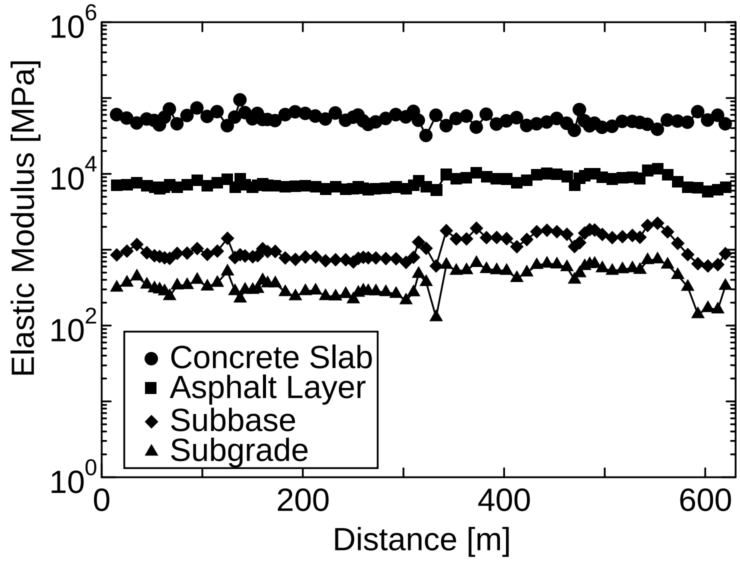


**Figure 8. Variations of Estimated Moduli along Distance for Section A.**

**Table 3. Statistic Parameters of Estimated Moduli for Section A.**

| | Concrete | Asphalt | Subbase | Subgrade |
|---|---|---|---|---|
| | | A all | | |
| Average (MPa) | 5.30E+04 | 7.74E+03 | 1.11E+03 | 4.00E+02 |
| Standard Deviation.(MPa) | 9.62E+03 | 1.37E+03 | 4.11E+02 | 1.56E+02 |
| COV (%) | 18 | 18 | 37 | 39 |
| | | A-1 | | |
| Average (MPa) | 5.60E+04 | 6.97E+03 | 8.67E+02 | 3.12E+02 |
| Standard Deviation.(MPa) | 1.01E+04 | 5.76E+02 | 1.51E+02 | 6.73E+01 |
| COV (%) | 18 | 8 | 17 | 22 |
| | | A-2 | | |
| Average (MPa) | 4.83E+04 | 9.11E+03 | 1.54E+03 | 5.64E+02 |
| Standard Deviation.(MPa) | 7.01E+03 | 1.12E+03 | 3.09E+02 | 9.59E+01 |
| COV (%) | 15 | 12 | 20 | 17 |

## Backanalysis

***Method.*** Backanalysis was performed for the FWD deflections to estimate stiffness moduli of pavement layers. The program employed in this study was BALM99 that was developed by Matsui et al. (2000). The program utilizes the multi-elastic-layer model in the forward process and Gauss-Newton algorithm with truncated singular value decomposition in the backward process. In the analysis, a four-layered system with a concrete slab, asphalt interlayer, granular subbase and subgrade was assumed. The thickness of each layer was the same as in **Table 1**, and their Poisson's ratios were assumed 0.2 and 0.35 for concrete slab and the rest of the underlying layers, respectively. The interface condition between the concrete slab and the asphalt interlayer was assumed as smooth (no-bonding between them).

Another method is a dynamic one, where backanalysis was implemented by axi-symmetric analysis of multi-layered elastic system using finite element method (FEM) procedure (Matsui *et al.* 2003). A mathematical model for dynamic analysis of pavement due to impulsive force is formulated using 8-nodes isoparametric elements. This usually results in large degrees of freedom and computational time becomes enormous particularly when the system of equations has to be solved repeatedly. However, Ritz vectors for matrix reduction (Wilson et al., 1982) were employed in order to improve computational efficiency without losing accuracy. Gauss-Newton method with truncated singular value decomposition was also used in the backanalysis.

## Estimated Moduli in Section A

**Figure 8** shows variations of the estimated moduli of Section A along the distance. The variations of the moduli of the concrete slab and asphalt interlayer were small and uniform, while there was clear a distinction in the moduli of granular subbase and subgrade between A-1 and A-2.

**Table 3** summarizes statistic parameters of the estimated moduli in Section A. Differences in COV of the concrete slab and interlayer between Sections A, and the subsections, A-1 and A-2 were very small. On the other hand, COVs of subbase and subgrade in the subsections A-1 and A-2 were less than that in Section A, suggesting that the structural difference between A-1 and A-2 was due to moduli of the subbase and subgrade. COVs of the estimated moduli of a sound pavement structure in a uniform section might be less than 20 %.

**Figure 9** shows a histogram of estimated modulus of concrete in Section A. The frequency distribution has only one peak and can be approximated by a normal probability distribution function, suggesting that the estimated modulus of concrete is uniform.

**Figures 10 (a)** to **10 (c)** show histograms of the estimated subgrade moduli for the entire section and the subsections, A-1 and A-2, respectively. The frequency for the entire section has two peaks as shown in **Figure 10 (a)**. For each subsection, the frequency has only one peak and can be approximated by a normal distribution as shown **Figures 10 (b)** and **10 (c)**, suggesting, again, that the difference between A-1 and A-2 might be due to the difference in modulus between subbase and subgrade.

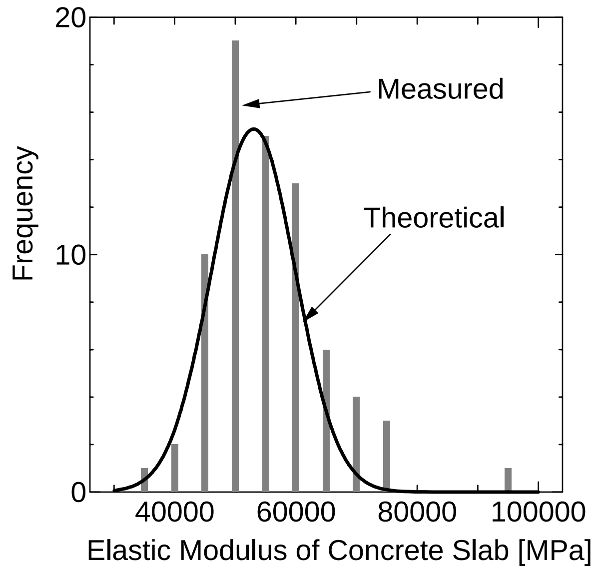


**Figure 9. Histogram of Elastic Modulus of Concrete for Section A.**

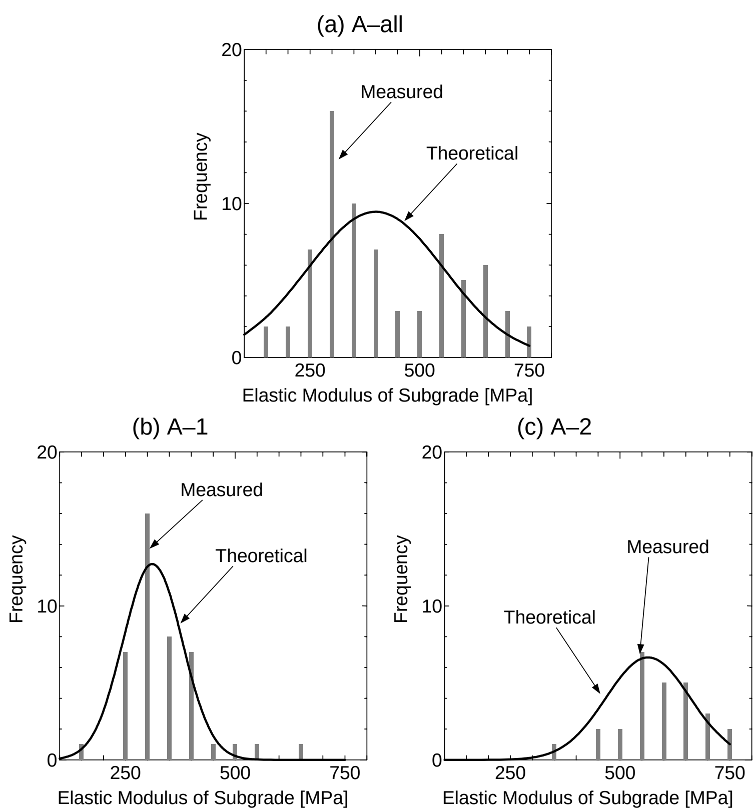


**Figure 10. Histograms of Elastic Modulus of Subgrade for Section A**

**Table 4. Range of Values for Generation of Seed Layer Moduli.**

| Layer | Range of Value Used (MPa) |
|---|---|
| Concrete Slab | 19613 < E1 < 39226 |
| Asphalt Interlayer | 1961 < E2 < 7845 |
| Granular subbase | 98 < E3 < 490 |
| Subgrade | 9 < E4 < 98 |

**Table 5. Results of Dynamic Backanalysis.**

| Layer | Average Layer Moduli (MPa) | Standard Deviation (MPa) | Coefficient of Variation (%) |
|---|---|---|---|
| Concrete Slab | 38,000 | 552 | 1.5 |
| Asphalt Interlayer | 6,900 | 821 | 12.0 |
| Granular subbase | 300 | 124 | 41.6 |
| Subgrade | 200 | 4 | 1.8 |

## Dynamic Backanalysis

In order to investigate the influence of seed values on the backcalculated layer moduli, 100 random numbers were used to generate 100 sets of seed values for layer moduli. The range of seed moduli for each layer is as shown in **Table 4**. Seed layer moduli developed were then used in dynamic backanalysis and results obtained are shown in **Table 5**. With the exception of the granular subbase whose layer modulus is considered to be low, the average results obtained for the other layers are considered to be reasonable bearing in mind this was a newly constructed section. COV of layer moduli are also within the acceptable range, again with the exception of the granular subbase. CBR of the subgrade was set at 12% in the design phase, and this value matches well with the backcalculated layer modulus of 200 MPa that was obtained. This is an indication that dynamic backanalysis may give results that are within the acceptable range.

Comparing with results obtained using static backanalysis, layer moduli by dynamic analysis were small. This difference may be attributed to the fact that the interface condition between the concrete slab and the asphalt interlayer was assumed to be rough (complete bonding between them), which is different from the condition considered during static analysis. The other factor should be the modeling differences between static and dynamic methods.

## Conclusions

Statistical characteristics of FWD deflections and the backcalculated moduli were investigated based on the data obtained with FWD tests conducted on the newly constructed concrete pavements. The precise statistical evaluation can be done for uniform section that can be identified by AASHTO method. COV of FWD deflection in a uniform section would be about 10 to 20 %. That of LTE would be less than 10 % in sound doweled joints. By back- analyzing the FWD deflections, the effect of thickness of concrete slab could be eliminated. COV of backcalculated moduli ranged from 10 to 20 % for a uniform section. Since the modulus of concrete slab was almost uniform, the difference in FWD deflections among the subsections might come from the difference in the subbase and subgrade moduli.

When random numbers were used to generate seed values for backanalysis, it was realized that differences in seed layer moduli could lead to very different backanalyzed results. This implies the use of several sets of randomly selected seed layer moduli to compute mean backanalyzed results is recommended for more reliable pavement layer moduli.

## Acknowledgments

The authors would like to acknowledge the support by Research Institute of Technology, Tokyo Denki University (Project No. Q02M-05) and Program for Promoting Fundamental Transport (Project No. 2000-03).

## References

American Association of State Highway Officials (1986). *AASHTO Guide for Design of Pavement Structures*.

Matsui, K., Kurobayashi, I., and Nishiyama, D. (2000). "Examination on Improvement of Accuracy for Elastic Modulus from FWD Test." *Journal of Pavement Engineering, Japan Society for Civil Engineers*, Vol.5, pp.139-147.

Matsui, K., Maina, J. W., Dong, Q., and Sasaki, Y. (2003). "A Fast Dynamic Backcalculation of Layer Moduli using Axi-Symmetric Approach." *International Journal of Pavements*, Volume 2 Number 1-2, pp. 75 – 87.

Wilson, E.L., Yuan, M. W., Dicken, J. M. (1982). "Dynamic analysis by direct superposition of Ritz vectors." *Earthquake Engineering and Structural Dynamics* Vol.10, pp. 813-821.